UNEC Journal of Engineering and Applied Sciences
Vol. 5, No.2, 2025, pp. 116-126
DOI: https://doi.org/10.61640/ujeas.2025.1211

SECTION:
CHEMISTRY &
MATERIALS SCIENCE

Synthesis and crystal structure of benzo[*b*]thiophen-2-ylgold(I) *tert*-Butyl Isocyanide

O.V. Repina[1], A.I. Korolev[1], A.S. Kubasov[2], A.G. Tskhovrebov[1*], N.Q. Shikhaliyev[3], A.A. Niyazova[4], M. Akkurt[5]

[1]Peoples' Friendship University of Russia, 6 Miklukho-Maklaya Street, Moscow 117198, Russian Federation
[2]Kurnakov Institute of General and Inorganic Chemistry, RAS, 31 Leninsky Prosp., 119991 Moscow, Russian Federation
[3]Department of Chemical Engineering, Baku Engineering University, Khirdalan city, 120 Hasan Aliyev str., Baku AZ0101, Azerbaijan
[4]Department of Engineering and Applied Sciences, Azerbaijan State University of Economics (UNEC), 6 Istiglaliyyat str, Baku AZ1001, Azerbaijan
[5]Department of Physics, Faculty of Sciences, Erciyes University, Kayseri 38039, Turkey
email: *alexander.tskhovrebov@gmail.com*

Abstract

A novel benzo[b]thiophen-2-ylgold(I) tert-butyl isocyanide complex was synthesized via a facile transmetallation reaction from the corresponding boronic acid. Single-crystal X-ray diffraction analysis revealed that the complex forms a zigzag-shaped tetramer in the solid state, stabilized by aurophilic interactions (Au···Au 3.1585(4) and 3.1837(6) Å). The supramolecular architecture is further supported by a combination of S···H contacts and CH–π interactions, resulting in a stable three-dimensional network.

***Keywords*:** crystallization, supramolecular features, CH–π interactions, benzo[b]thiophen-2-ylgold(I) tert-butyl isocyanide, transmetallation reaction.

PACS numbers: 61.50.−f,61.10.Nz

Received:	*Revised:*	*Accepted:*	*Published:*
5 June 2025	*23 August 2025*	*16 December 2025*	*30 December2025*

1. Introduction

Organogold(I) chemistry, particularly complexes featuring isocyanide ligands, has been a field of active research for over half a century [1-4]. These compounds are of significant interest due to their diverse applications, notably as phosphorescent materials [5-8] and efficient catalysts in organic synthesis [9-13]. The Lewis acidic nature of the gold(I) center and its carbophilicity is key to its reactivity, enabling the activation of unsaturated substrates such as isocyanides, which serve as classic σ-donor ligands in coordination chemistry.

The conventional synthetic route to aryl gold(I) isocyanide complexes relies on the transmetallation from organomagnesium reagents [8,14], a method often complicated by anhydrous conditions and the sensitivity of the reagents. In contrast, transmetallation from boronic acids [11,12,15] presents a more robust and versatile alternative, a reaction step also identified as a key intermediate in gold-catalyzed Sonogashira-type couplings. This boronic acid pathway potentially facilitates access to a wider range of functionalized aryl complexes, enabling the systematic exploration of structure-property relationships.

While the molecular structures of such complexes are often linear, their solid-state

supramolecular architectures are dictated by weak, yet highly influential, non-covalent interactions. Among these, aurophilic interactions [4,16,17] are a hallmark of gold(I) chemistry and are known to profoundly impact photophysical properties [18,19]. However, the predictable formation of specific oligomeric species, such as discrete tetramers, through a combination of aurophilic and other weak forces remains an area of keen interest.

In this context, we report the synthesis and detailed structural analysis of a novel benzo[b]thiophen-2-yl gold(I) tert-butyl isocyanide complex. Utilizing the practical boronic acid transmetallation route, we obtained the target complex and uncovered its solid-state structure.

2. Synthesis and crystallization

The title compound was prepared according to a literature procedure[15](figure 1). Chloro(dimethyl sulfide)gold(I) (15.0 mg, 0.051 mmol, 1.0 eq) and tert-butyl isocyanide (4.2 mg, 0.051 mmol, 1.0 eq) were dissolved in dichloromethane (2 ml) in a 10 ml vial equipped with a magnetic stir bar. Benzo[b]thiophene-2-boronic acid (9.1 mg, 0.051 mmol, 1.0 eq) was dissolved in methanol (2 ml) and added to a solution under stirring, then sodium carbonate (54.0 mg, 0.51 mmol, 10 eq) was added. After 1 hour of stirring the mixture was filtered, the solution was evaporated and the residue was purified by column chromatography (eluent: DCM/hexane, 1:1), then evaporated and dried under vacuum. White solid. Yield: 7.8 mg (37%). Crystals suitable for X-ray analysis were obtained by layering hexane over a dichloromethane solution of the target complex.

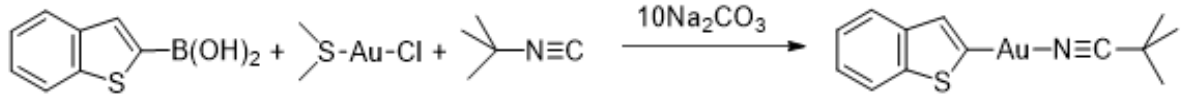

Figure 1. Synthesis of the title gold(I) complex

3. X-ray single crystal crystallography

A suitable single crystal was carefully selected and mounted on a glass fiber prior to data acquisition. Diffraction data were collected using a Bruker SMART APEX II diffractometer equipped with Mo-Kα radiation (λ = 0.71073 Å) at ambient temperature. Standard corrections for Lorentz, polarization, and absorption effects were applied to the collected intensities. The crystal structure was determined employing direct methods as implemented in the SHELXT [24] program and subsequently refined using full-matrix least-squares procedures on F^2 within the SHELXL [25] framework. Hydrogen atoms were placed in calculated positions and refined using a riding model, with C–H distances of 0.95–0.98 Å and U_{iso}(H) values set to 1.5 U_{eq}(C) for methyl groups and 1.2 U_{eq}(C) for aromatic carbon atoms.

The thiophene ring (S2/C19–C22) in molecule **II** is rotationally disordered (flip disorder) by *ca* 180° (around the single C14—Au2 bond, to which it is attached) over two sites with the site-occupation factors of 0.55 and 0.45 (fixed after refinement cycles). For these rings, FLAT, SADI and EADP instructions were also used. Due to weak agreement between the measured and calculated intensities, nineteen reflections were excluded from the final refinement. (0 1 1, 0 -1 1, -15 8 2, -14 10 6, -12 9 -7, -8 2 12, -11 2 6, -1 6 16, 2 -2 -14, -7 7 16, -3 -3 -3, -3 -17 -1, -13 9 -3, -11 9 7, 1 6 -2, -2 0 -16, 4 2 -17, 0 11 11, 11 2 -8) were omitted during the final refinement cycle. ORTEP-3 [26] and Platon [29] software was used for graphics. The experimental parameters and their particulars are itemized in table 1.

CCDC number	2503130
Chemical formula	$C_{13}H_{14}AuNS$
M_r	413.28
Crystal system, space group	Monoclinic, $P2_1/n$
Temperature (K)	150
a, b, c (Å)	12.9222 (8), 14.2309 (8), 14.6977 (9)
β (°)	101.526 (2)
V (Å^3)	2648.3 (3)
Z	8
Radiation type	Mo $K\alpha$
(mm^{-1})	11.24
Crystal size (mm)	0.20 × 0.10 × 0.04
Diffractometer	Bruker *SMART APEX* II
Absorption correction	Multi-scan *SADABS* [24] was used for absorption correction. wR2(int) was 0.1693 before and 0.0800 after correction. The Ratio of minimum to maximum transmission is 0.4728. The λ/2 correction factor is Not present.
T_{min}, T_{max}	0.353, 0.746
No. of measured, independent and observed [$I > 2\sigma(I)$] reflections	37031, 6324, 5024
R_{int}	0.094
$(\sin\theta/\lambda)_{max}$ (Å^{-1})	0.659
$R[F^2 > 2\sigma(F^2)]$, $wR(F^2)$, S	0.044, 0.084, 1.04
No. of reflections	6324
No. of parameters	290
No. of restraints	12
H-atom treatment	H-atom parameters constrained
$\Delta\rho_{max}$, $\Delta\rho_{min}$ (e Å^{-3})	1.18, −1.56

Table 1. Crystal data and structure refinement parameters for compounds 3a and 3c

4. Structural commentary and supramolecular features

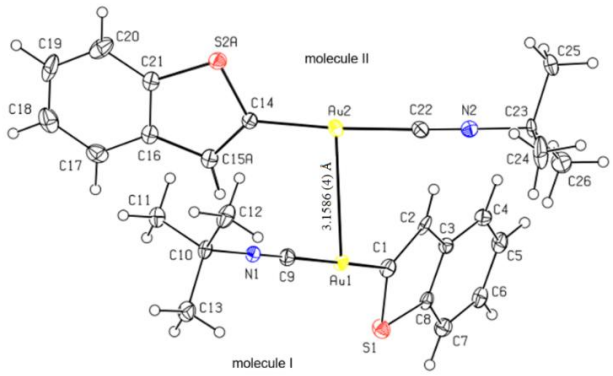

Figure 2. The molecular structure is shown with the corresponding atom numbering, and displacement ellipsoids are presented at the 30% probability level, while the minor disordered part is not displayed for clarity

The complex crystallizes in the monoclinic $P2_1/n$ space group with Z = 8 (figure 1). Figure 2 shows an overlay plot of two molecules in the asymmetric unit, with an r.m.s. deviation of 0.725 Å. Except for the atoms of the minor part of the disordered molecule and the butyl group, all atoms of two molecules are quite compatible and coincide with each other. The asymmetric unit contains one-half of the tetrameric molecule (figure 3), the center of which coincides with an inversion center.

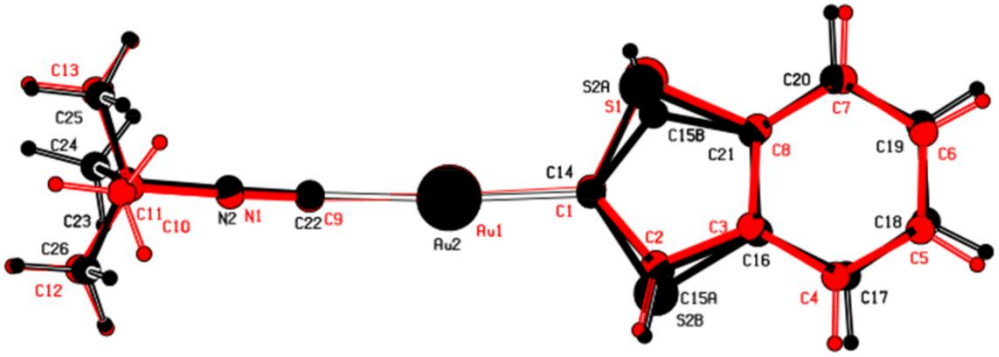

Figure 3. Overlay of two molecules present in the asymmetric unit

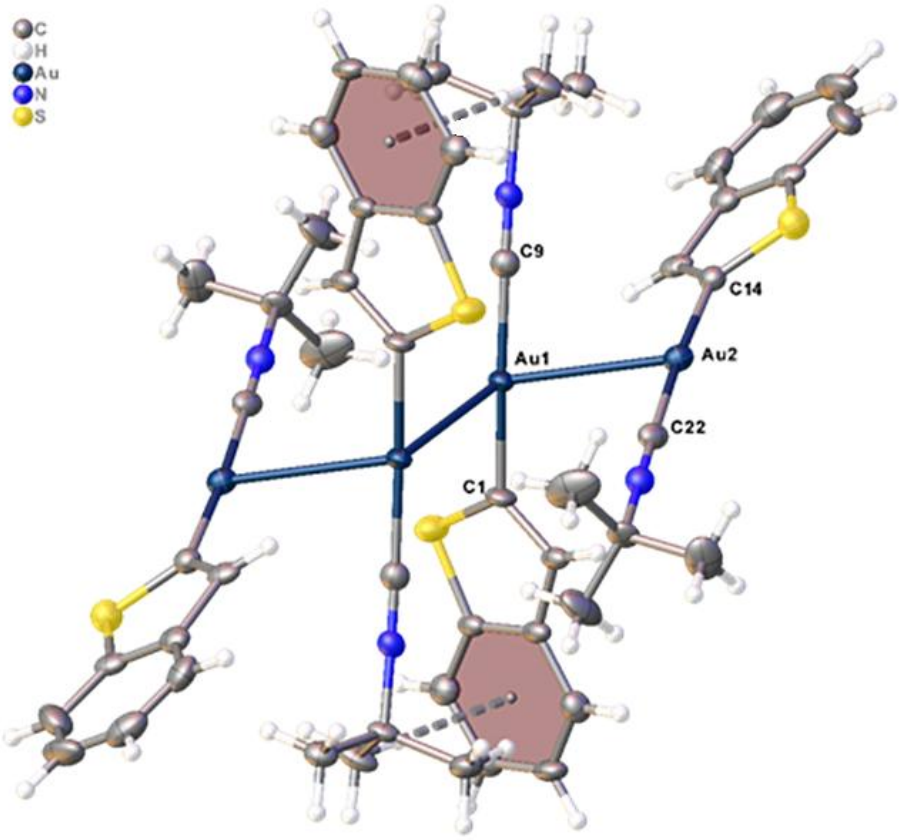

Figure 4. The molecular structure of the compound is shown with displacement ellipsoids drawn at the 50% probability level

The tetramer adopts a zigzag configuration, which is stabilized by aurophilic interactions between the gold atoms with Au···Au distances of 3.1586(4) and 3.1837(6) Å and an Au-Au-Au angle of 107.259(14)° (table 2). Each gold(I) center exhibits the typical linear coordination geometry, with C–Au–C angles of 175.6(3)° and 175.9(3)° (table 2). The Au–C bond lengths to the isocyanide and aryl carbon atoms are 1.991(8)/1.975(8) Å and

2.021(8)/2.023(8) Å, respectively (table 1). The central units of the tetramer are arranged in a strictly head-to-tail fashion, as evidenced by a C1–Au1···Au1'–C1' torsion angle of 180.0°. In contrast, the terminal fragments are oriented with a C1–Au1···Au2–C14 torsion angle of 114.2°. The stability of the tetrameric framework is further enhanced by a pair of C–H···π interactions (figure 4, table 3). The other bond lengths and angles are comparable to those in the similar structures discussed in a recently published study [25].

Au1—C9	1.991 (8)	S2A—C14	1.681 (7)
Au1—C1	2.021 (7)	S2A—C21	1.715 (8)
Au1—Au2	3.1586 (4)	S2B—C16	1.687 (9)
Au1—Au1^{i}	3.1837 (6)	S2B—C14	1.687 (8)
Au2—C22	1.975 (8)	N1—C9	1.139 (9)
Au2—C14	2.023 (8)	N1—C10	1.463 (8)
S1—C1	1.737 (8)	N2—C22	1.154 (9)
S1—C8	1.743 (7)	N2—C23	1.461 (9)
C9—Au1—C1	173.6 (3)	C1—S1—C8	92.9 (4)
C9—Au1—Au2	77.7 (2)	C14—S2A—C21	92.8 (4)
C1—Au1—Au2	102.4 (2)	C16—S2B—C14	92.2 (4)
C9—Au1—Au1^{i}	106.0 (2)	C9—N1—C10	175.3 (7)
C1—Au1—Au1^{i}	80.1 (2)	C22—N2—C23	178.4 (7)
Au2—Au1—Au1^{i}	107.259 (14)	C2—C1—S1	113.0 (5)
C22—Au2—C14	175.9 (3)	C2—C1—Au1	127.4 (5)
C22—Au2—Au1	88.2 (2)	S1—C1—Au1	119.4 (4)
C14—Au2—Au1	95.88 (17)		
Symmetry code: (i) −*x*+1, −*y*+1, −*z*+1.			

Table 2. Selected geometric parameters (Å, °)

Cg1, Cg2, Cg3 and Cg5 are the centroids of the major and minor parts S2A/C14/C15A/C16/C21 and S2B/C14/C15B/C21/C16 of the disordered thiophene ring, and the benzene rings C16-C21 and C3--C8, respectively				
D—H···*A*	*D*—H	H···*A*	*D*···*A*	*D*—H···*A*
C7—H7···S2A^{ii}	0.95	2.90	3.718 (9)	145
C17—H17···S2B^{iii}	0.95	2.96	3.682 (10)	134
C24—H24A···S2A^{iv}	0.98	3.01	3.932 (11)	158
C5—H5···Cg3^{v}	0.95	2.69	3.611 (8)	162
C11—H11A···Cg1	0.98	2.85	3.640 (9)	138
C11—H11A···Cg2	0.98	2.83	3.596 (9)	135
C12—H12A···Cg5^{i}	0.98	2.57	3.546 (9)	176
C26—H26B···Cg5^{v}	0.98	2.91	3.840 (10)	158
Symmetry codes: (i) −*x*+1, −*y*+1, −*z*+1; (ii) *x*−1/2, −*y*+1/2, *z*+1/2; (iii) −*x*+1, −*y*, −*z*+1; (iv) −*x*+3/2, *y*+1/2, −*z*+1/2; (v) −*x*+3/2, *y*+1/2, −*z*+3/2.				

Table 3. Hydrogen-bond geometry (Å, °)

In the crystal lattice, the tetramers are interconnected primarily via weak C–H···S hydrogen bonds (figures 5 to 8, table 2). Additional stabilization is provided by C–H···π contacts involving the central and terminal benzothiophene fragments of adjacent molecules (figure 6, table 3).

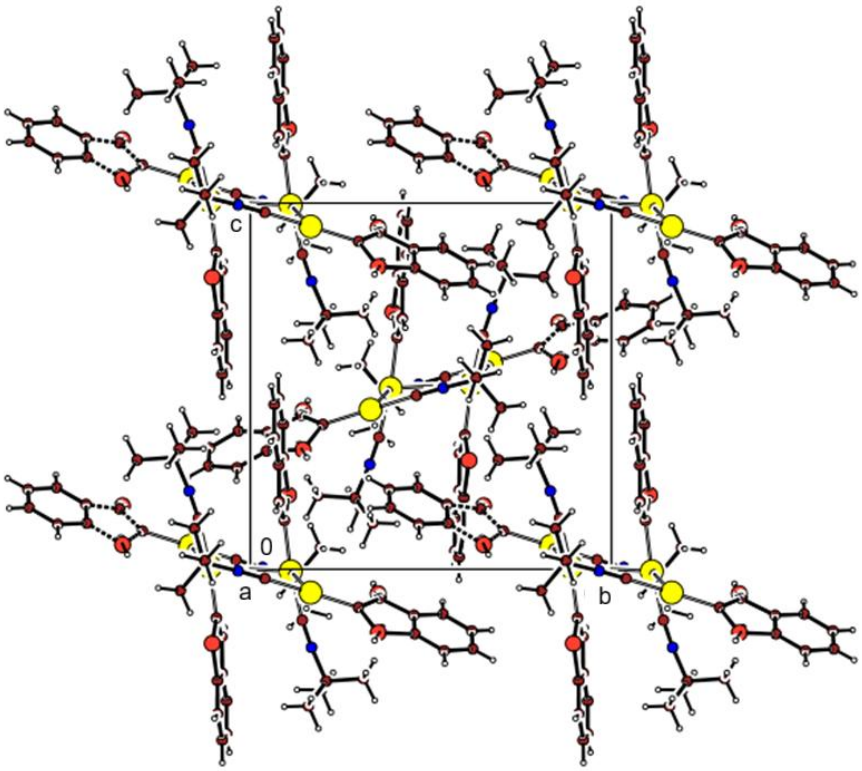

Figure 5. Molecular packing of the compound, viewed down the a axis

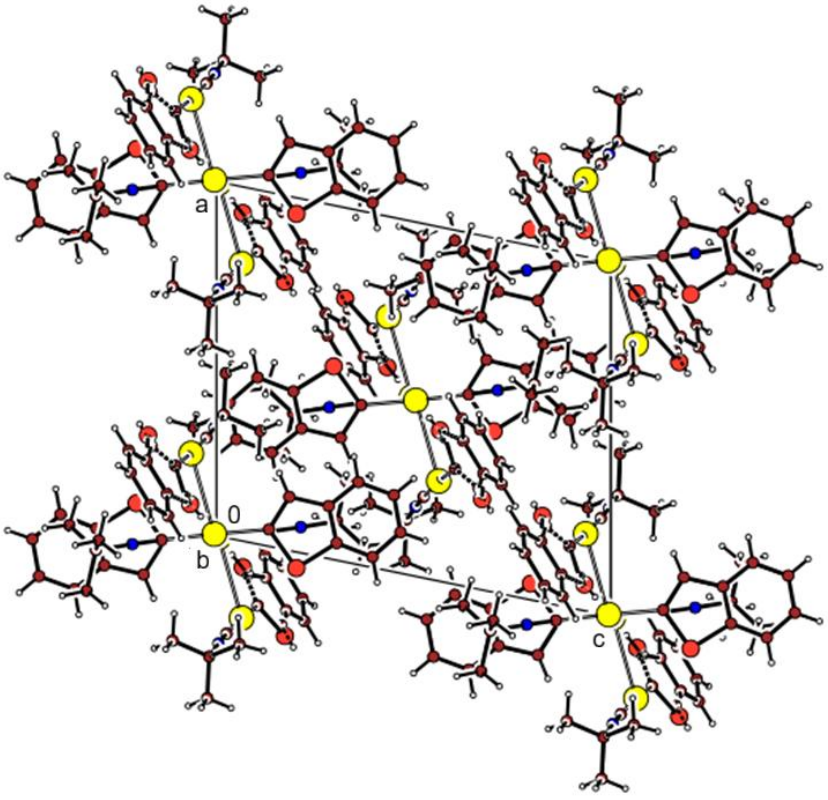

Figure 6. Molecular packing of the compound, viewed down the b axis

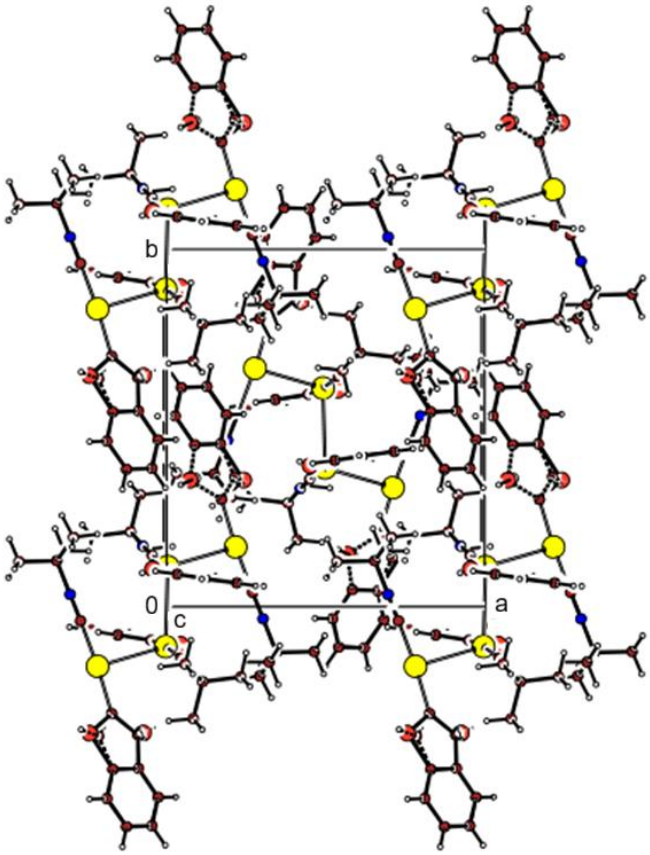

Figure 7. Molecular packing of the compound, viewed down the c axis

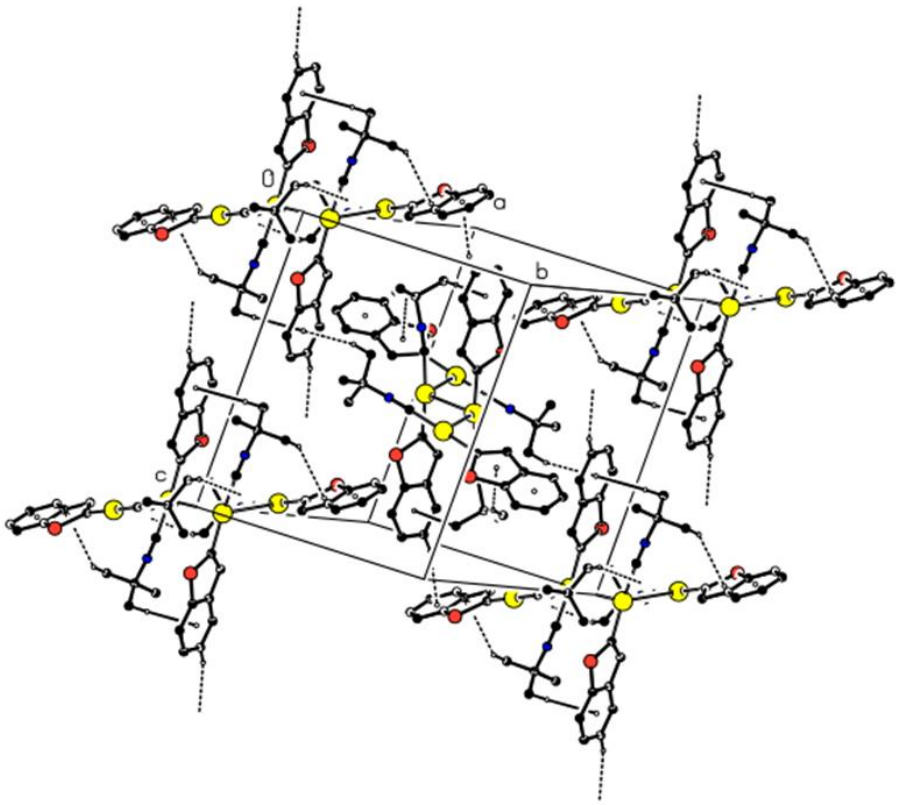

Figure 8. Partial view illustrating the C---H… π interactions within the unit cell

5. Hirshfeld surface analysis

Hirshfeld surfaces and two-dimensional fingerprint plots have been generated to visualize the intermolecular contacts of the compound using *Crystal Explorer* program [26]. These intercontacts are featured by normal mapping of d_{norm} on molecular Hirshfeld surfaces (figure 9a). The 3D Hirshfeld Surface mapped over d_{norm} between -0.1282 a.u (blue) and 1.3969 a.u (red). White denotes contacts with distances equal to the van der Waals (vdW) radii. Connections that are short of the vdW radii are represented in red, while those that exceed the vdW radii are shown in blue. In figure 7*a*, dark-red spots represent strong intermolecular C—H···S interactions. In addition, the shape-index is used to identify complementary hollows (red) and bumps (blue) where two molecular surfaces touch one another (figure 9b). This includes π–π stacking, represented by adjacent red and blue triangles. In this structure there are C---H… π interactions and no π–π stacking interaction. Curvedness is a tool for pinpointing planar stacking configurations and how neighbouring molecules interact. Figure 9c shows relatively large green planes in the nine-membered ring systems separated by blue edges. These green planes give us an idea of the flatness of complexes, and the fragment patch (figure 9d) is designed to indicate the nearest neighbouring molecule [7].

In the crystal structure of the compound, intermolecular C—H···S and C—H···π interactions were observed. The two-dimensional fingerprint plots show that the main contributors to crystal packing are H…H contacts (54.8 %, figure 10b), C…H/H…C (25.9 %, figure 10c), S…H/H…S (7.2 %, figure 10d) and Au…H/H…Au (6.0 %, figure 10e). The remaining small contributions are C…C (1.5 %), S…C/C…S (1.3 %), Au…C/C…Au (1.0 %), Au…Au (0.8 %), N…C/C…N (0.5 %), N…H/H…N (0.5 %), Au…N/N…Au (0.3 %), and S…N/N…S (0.2 %). The optimized molecular geometry corresponded well to the observed solid-state geometry. This supports the crystallographic findings and implies that the molecular structure is stable.

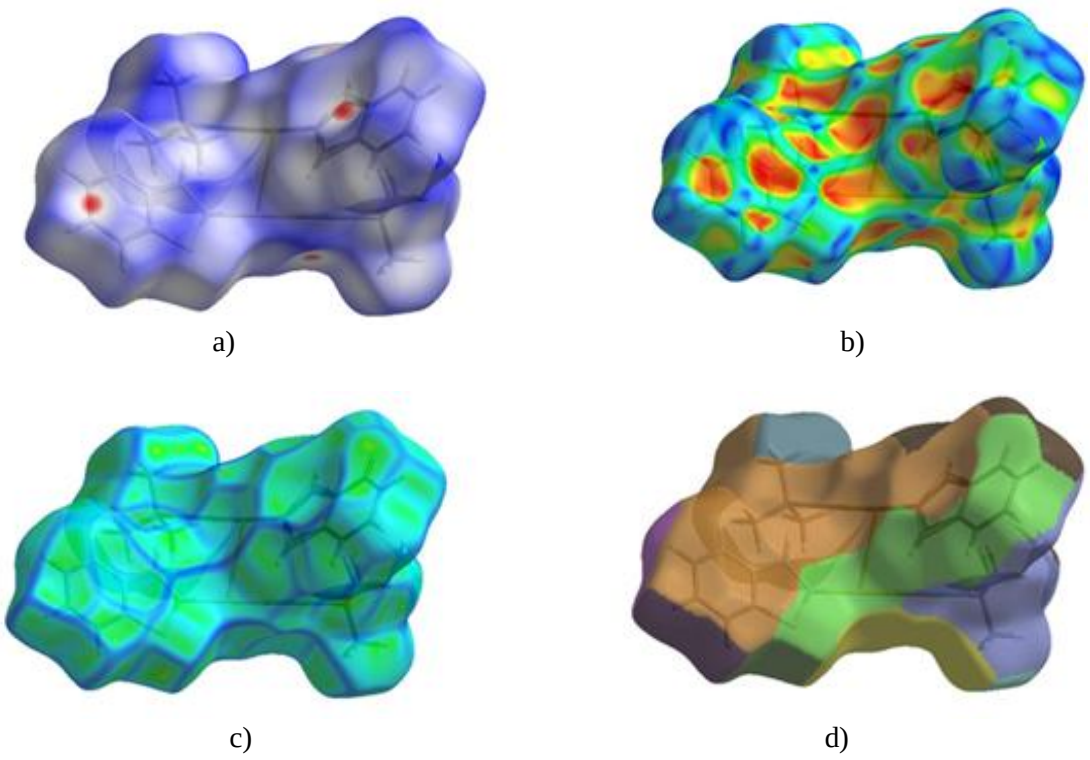

Figure 9. Hirshfeld surface mapped over dnorm for compound, showing intermolecular contacts. Hirshfeld surfaces for the compound mapped with a) dnorm b) shape index, c) curvedness, d) fragment patch for the compound

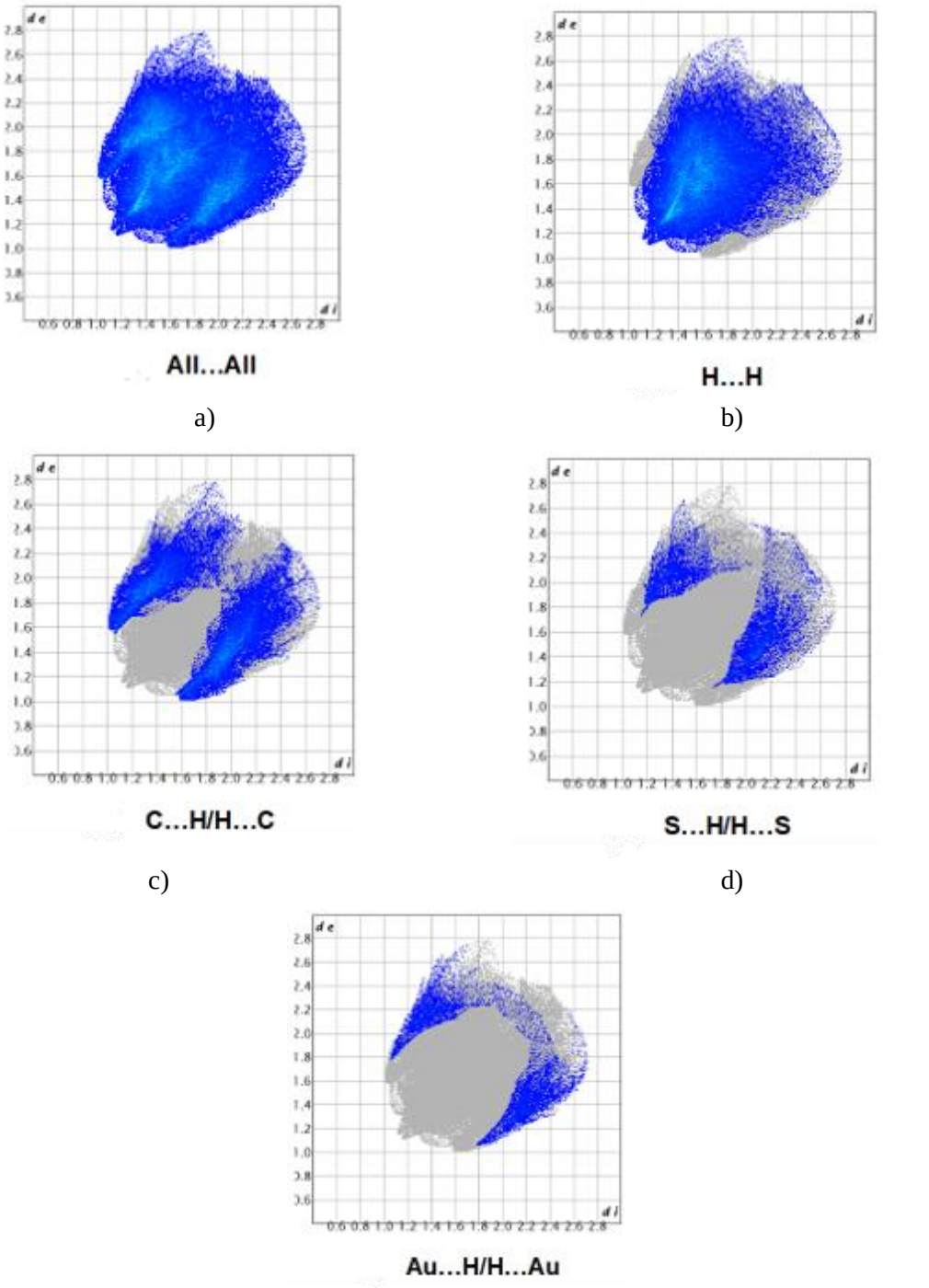

Figure 10. Two-dimensional fingerprint plots of compound, showing b) H…H, c) C…H/H…C, d) S…H/H…S, and e) Au…H/H…Au contacts. The complete fingerprint outline is indicated in grey, while di and de correspond to the nearest internal and external distances from a point on the Hirshfeld surface

6. Conclusion

In conclusion, we have successfully synthesized a novel benzo[b]thiophen-2-yl gold(I) tert-butyl isocyanide complex through a practical and robust transmetallation reaction from the corresponding boronic acid. This method offers a valuable alternative to the more sensitive organomagnesium-based routes, potentially broadening access to functionalized aryl gold(I) isocyanide complexes. Single-crystal X-ray diffraction analysis revealed that the complex does not exist as discrete monomers in the solid state but instead self-assembles into

a well-defined zigzag-shaped tetramer. This supramolecular architecture is primarily stabilized by significant aurophilic interactions (Au···Au 3.1586(4) - 3.1837(6) Å), which dictate the tetrameric arrangement.

Appendix A. Supplementary data

Supplementary crystallographic data for this article in CIF format are available at the Electronic Supplementary Publication from Cambridge Crystallographic Data Centre (CCDC **2503130**). This data can be obtained free of charge via http://www.ccdc.cam.ac.uk/conts/retrieving.html, from the Cambridge Crystallographic Data Centre, 12 Union Rood, Cambridge CB2 1EZ, UK (Fax: (international): +44 1223/336 033; e-mail: deposit@ccdc.cam.ac.uk).

Funding

This work was performed with the support of the Russian Science Foundation (award No. 25-23-00043). Theoretical studies were supported by the RUDN University 021341-2-000.

References

1. H. Ecken, M.M. Olmstead, B.C. Noll, S. Attar, B. Schlyer, A. L. Balch, Journal of the Chemical Society, Dalton Transactions **22** (1998) 3715.
2. G. Jia, N.C. Payne, J.J. Vittal, R.J. Puddephatt, Organometallics **12**(12) (1993) 4771.
3. R. Usón, A. Laguna, J. Vicente, J. García, B. Bergareche, P. Brun, Inorganica Chim Acta **28** (1978) 237.
4. N.Q. Shixaliyev, A.M. Maharramov, A.V. Gurbanov, N.V. Gurbanova, V.G. Nenajdenko, V.M. Muzalevskiy, K.T. Mahmudov, M.N. Kopylovich, Journal of Molecular Structure **1041** (2013) 213.
5. M.V. Grudova, A.S. Novikov, A.S. Kubasov, V.N. Khrustalev, A.A. Kirichuk, V.G. Nenajdenko, A.G. Tskhovrebov, Crystals (Basel) **12**(5) (2022) 613.
6. H. Ito, T. Seki, Bull Jpn Soc Coord Chem 62 (2013) 3.
7. T. Seki, N. Tokodai, S. Omagari, T. Nakanishi, Y. Hasegawa, T. Iwasa, T. Taketsugu, H. Ito, J Am Chem Soc **139**(19) (2017) 6514.
8. S. Coco, C. Cordovilla, P. Espinet, J. Martín-Álvarez, P. Muñoz, Inorg Chem **45**(25) (2006) 10180.
9. J. Wang, Z.-Y. Wang, P. Luo, B. Li, L.-Y. Wang, S.-Q. Zang, Crystal Growth & Design **19**(2) (2019) 538.
10. Y. Xu, X. Hu, J. Shao, G. Yang, Y. Wu, Z. Zhang, Green Chemistry **17**(1) (2015) 532.
11. A.R. Asgarova, A.N. Khalilov, I. Brito, A.M. Maharramov, N.G. Shikhaliyev, J. Cisterna, A. Cárdenas, A.V. Gurbanov, F.I. Zubkov, K.T. Mahmudov, Acta Crystallographica Section C Structural Chemistry **75** (2019) 342.
12. K. Özkaraca, M. Akkurt, N.Q. Shikhaliyev, U.F. Askerova, G.T. Suleymanova, G.Z. Mammadova, D.M. Shadrack, Acta Crystallographica Section E Crystallographic Communications **76** (2020) 1251.
13. A. Ribeiro, I. Matias, P. Zargaran, A. Hashmi, L. Martins, Materials **14** (2021) 4294.
14. L. Zhang, W. Zhang, D. Li, R. Yang, Z. Xia, iScience **27**(1) (2024) 108531.
15. S. Zhang, X. Ye, L. Wojtas, W. Hao, X. Shi, Green Synthesis and Catalysis **2**(1) (2021) 82.
16. D.S. Bolotin, N.A. Bokach, A.S. Kritchenkov, M. Haukka, V.Yu. Kukushkin, Inorganic Chemistry 52(11) (2013) 6378.
17. X. Deng, S. Liu, C. Fan, H. Liu, Y. Zou, H. He, D. Deng, S. Pu, Z. Chen, Spectrochimica Acta Part A: Molecular and Biomolecular Spectroscopy **321** (2024) 124712.
18. K. Ozkaraca, M. Akkurt, N.Q. Shikhaliyev, U.F. Askerova, G.T. Suleymanova, I.M. Shikhaliyeva, A. Bhattarai, Acta Crystallographica Section E **76** (2020) 811.

19. K.G. Pavlov, M.R. Grudova, A.S. Kubasov, V.N. Khrustalev, I.S. Kritchenkov, R.M. Gomila, A. Frontera, A.G. Tskhovrebov, CrystEngComm **27** (2025) 7021.
20. A.G. Tskhovrebov, A.S. Novikov, A.S. Kritchenkov, V.N. Khrustalev, M. Haukka, Zeitschrift für Kristallographie **235**(10) (2020) 477.
21. A.G. Tskhovrebov, A.S. Novikov, B.S. Tupertsev, A.A. Nazarov, A.A. Antonets, A.A. Astafiev, A.S. Kritchenkov, A.S. Kubasov, V.G. Nenajdenko, V.N. Khrustalev, Inorganica Chimica Acta **522** (2021) 120373.
22. R.L. White-Morris, M.M. Olmstead, A.L. Balch, Journal of the American Chemical Society **125**(4) (2003) 1033.
23. X.-Y. Zhai, L. Zhao, Nature Communications **16**(1) (2025) 405.
24. G.M. Sheldrick, Acta Crystallographica A **71** (2015) 3.
25. G.M. Sheldrick, Acta Crystallographica C **71** (2015) 3.
26. L.J. Farrugia, Journal of Applied Crystallography 45 (2012) 849.
27. A.L. Spek, Acta Crystallographica E 76 (2020) 1.
28. Bruker, SADABS, Bruker AXS LLC, Madison, Wisconsin, USA (2016).
29. K.G. Pavlov, M.R. Grudova, A.S. Kubasov, V.N. Khrustalev, I.S. Kritchenkov, R.M. Gomila, A. Frontera, A.G. Tskhovrebov, CrystEngComm 27 (2025) 7021.
30. P.R. Spackman, M.J. Turner, J.J. McKinnon, S.K. Wolff, D.J. Grimwood, D. Jayatilaka, M.A. Spackman, Journal of Applied Crystallography **54** (2021) 1006.